

The University of Maine

DigitalCommons@UMaine

---

Honors College

---

Spring 2015

## Functionalization of Nanocellulose Fibers For Use In Radical Reactions

Thomas McOscar

University of Maine - Main, tmcoscar@gmail.com

Follow this and additional works at: <https://digitalcommons.library.umaine.edu/honors>

 Part of the [Chemistry Commons](#)

---

### Recommended Citation

McOscar, Thomas, "Functionalization of Nanocellulose Fibers For Use In Radical Reactions" (2015).  
*Honors College*. 237.

<https://digitalcommons.library.umaine.edu/honors/237>

This Honors Thesis is brought to you for free and open access by DigitalCommons@UMaine. It has been accepted for inclusion in Honors College by an authorized administrator of DigitalCommons@UMaine. For more information, please contact [um.library.technical.services@maine.edu](mailto:um.library.technical.services@maine.edu).

FUNCTIONALIZATION OF NANOCELLULOSE FIBERS  
FOR USE IN RADICAL REACTIONS

by

Thomas McOscar

A Thesis Submitted in Partial Fulfillment  
of the Requirements for a Degree with Honors  
(Chemistry)

The Honors College

University of Maine

May 2015

Advisory Committee:

William Gramlich, Assistant Professor of Chemistry, Advisor

William DiSisto, Professor of Chemical Engineering

Brian Frederick, Associate Professor of Chemistry

Carl Tripp, Professor of Chemistry

Kathleen Ellis, Adjunct Assistant Professor in Honors (English)

## **Abstract**

Plastics and polymers comprise an expansive and growing portion of the materials in consumer products. The field of renewable and biodegradable polymers offers an appealing opportunity to continue developing plastics and materials along with an alternative to petroleum-based products that can have damaging environmental effects. Cellulose, the most abundant biological polymer on Earth, is an especially intriguing material for its diverse physical properties, its mass abundance, and the chemistry it can undergo, becoming a platform for other materials and reactions. On its smallest mechanical scale, the material becomes cellulose nano fibers.

The reaction between nanofibers of cellulose and methacrylic anhydride was studied using an aqueous basic suspension. The methacrylic anhydride was shown to react with cellulose to attach methacrylate groups to the surface of the nanofibers. The concentration of methacrylic anhydride was shown to have an effect on the degree to which the reaction progressed on the surface with higher concentrations leading to more reacted surfaces. There appeared to be a point where higher concentrations of methacrylic anhydride did not further react surfaces.

Methacrylate groups on the surface of cellulose provide interesting opportunities to propagate radical reactions from the surface. These reactions could provide mechanisms for cross-linking cellulose networks or adding other functional groups or polymer materials. The reaction also helps us to understand the nature of cellulose surfaces and the reactions it can support.

## Table of Contents

List of Figures .....	v
List of Tables .....	vii
1. Introduction .....	1
1.1 Renewable Polymers .....	1
1.2 Cellulose's .....	1
1.3 Nanocellulose .....	5
1.4 Applications and Reactions of Nanocellulose .....	6
1.5 Motivation for This Project .....	11
1.6 This Project .....	13
2. Experimental Methods for Functionalized Cellulose .....	15
2.1 Materials .....	15
2.2 Functionalizing Cellulose Workup .....	16
2.3 Control Nanocellulose Workup .....	17
2.4 Dialysis, Freeze-drying, Preparation for FTIR .....	17
2.5 Water Adsorption Effect on FTIR .....	18
2.6 Contaminant Isolation .....	19
2.7 FTIR Analysis and Integrations .....	20
2.7.1 Integration Macro .....	21
2.7.2 Peak Height Analysis .....	22
3. Results and Analysis .....	24
3.1 Analysis of Reaction Products .....	26

3.1.1 Treatment with Methacrylic Anhydride .....	26
3.1.2 Redialysis Control of Uncontaminated Material .....	28
3.2 Unreacted Nanocellulose .....	31
3.2.1 Prepared in Base .....	31
3.2.2 Rehydrated by Water Vapor .....	32
3.3 Investigations on Contaminated Functionalized Nanocellulose .....	36
3.3.1 Identifying Contaminants .....	36
3.3.2 Collecting and Characterizing Contaminants .....	38
3.4 Distinct Functionalized Products .....	39
3.5 Other Factors .....	41
3.5.1 Time Reacted .....	42
3.5.2 Reaction Temperature .....	43
3.6 Limitations of Analysis .....	44
3.7 Speculations on Reaction Extent .....	45
4. Conclusions .....	47
4.1 Results of Experiments .....	47
4.2 Future Works .....	48
4.2.1 Refinement of This Process .....	48
4.2.2 The Next Steps .....	49
References .....	50
Author Biography .....	52

## **List of Figures**

- 1.1: Structure of Cellulose
- 1.2: Cellulose's intramolecular hydrogen bonds
- 1.3 Cellulose's intermolecular hydrogen bonds
- 1.4: Conceptual structure of nanocellulose fibers
- 1.5: Structure of 6-acetoxy cellulose
- 1.6: Structure of Cellulose Nitrate
- 1.7: Simplified reaction producing carboxymethyl cellulose
- 1.8: Simplified reaction of TEMPO oxidation
- 1.9: Structure of Polylactic Acid
- 1.10: Structure of Polyisoprene
- 1.11: Conceptual structure of cellulose core-shell copolymer
- 2.1: Integration regions of sample infrared spectrum
- 2.2: Integration Methods of infrared spectrum
- 2.3: Height measuring regions and method of infrared spectrum
- 3.1: FTIR spectra control nanocellulose
- 3.2: FTIR spectra nanocellulose reacted with 60 mM methacrylic anhydride
- 3.3: Integrated comparison before/after extended dialysis
- 3.4: Peak height comparison before/after extended dialysis
- 3.5: FTIR spectra unreacted nanocellulose prepared in base
- 3.6: FTIR spectra nanocellulose exposed to atmosphere 15 minutes
- 3.7: FTIR spectra nanocellulose exposed to atmosphere 135 minutes

- 3.8: FTIR spectra nanocellulose exposed to saturated atmosphere 20 minutes 70°C
- 3.9: FTIR spectra nanocellulose with contaminant peak
- 3.10: FTIR spectra nanocellulose after redialysis removing contaminant peak
- 3.11: HNMR spectrum contaminant isolated from reacted cellulose
- 3.12: Average relative peak areas by reaction condition
- 3.13: Average maximum reaction temperatures and run times by reaction condition
- 3.14: Side reaction between methacrylic anhydride and water
- 3.15: Average reaction time by condition
- 3.16: Average reaction temperature by condition

## **List of Tables**

3.1: Integration results from all reaction samples

3.2: Calculations defining differences between integrations of reaction conditions

## **1. Introduction**

### **1.1 Renewable Polymers**

Plastics and composite materials are common in society both in engineering applications and in consumer products. Plastics can be found incorporated into many goods both in bottle and film/bag/wrap form. With plastics becoming common in an everyday setting, the environmental repercussions of plastics grow.

Recycling programs exist in many places for portions of materials, but in at least some cases a majority of a material can escape a recycling program<sup>1</sup>. In these instances, a more environmentally responsible approach would be to develop products made from biodegradable materials that would not pose any threats to the environment if released. Materials would also ideally be renewable, so that finite resources are not depleted. Developing materials that are both renewable and biodegradable doesn't necessarily remove the recycling process, but it could reduce the environmental impact of the materials that don't get recycled.

### **1.2 Cellulose**

Cellulose is a carbohydrate polymer made up repeating glucose monomers in pyranose form (glucopyranose) as shown in Fig 1.1. The monomers are linked together via  $\beta$ -1-4 linkages connecting the C-1 and C-4 carbons. All rings assume (with anomalous exceptions) the chair conformation with all functional groups in the equatorial position. Cellulose molecules are typically on the order of 1,000 to 15,000 glucose units long, though they vary by natural source. Cellulose fibers obtained from wood are up to 10,000 units long, including a wide distribution. Longer chains may be obtained from

cotton or hemp, which contains cellulose chains 10,000 to 15,000 units long<sup>2</sup>. Cellulose chains can be broken down by hydrolysis reactions that can occur under acidic or basic conditions<sup>3</sup>, so a cellulose stock of a particular length could be treated to form smaller fibers.

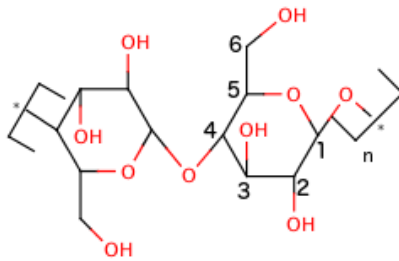


Fig 1.1: Cellulose: a polymer of  $\beta$ -1-4-linked glucopyranose that can form chains 1000 to 10,000 units long. Carbons are numbered in their conventional order.

Glucopyranose naturally has five hydroxyl groups: those bonded to carbons 1 through 4, and carbon 6 (C-1, C-2, C-3, C-4, C-6). The hydroxyls on C-1 and C-4 are not present in cellulose, as they have been converted into ethers. While some side reactions can occur where cellulose is bound to hemicelluloses or to lignin<sup>3</sup>, the remaining three hydroxyls are generally unaffected in cellulose, leaving two secondary hydroxyls (C-2, C-3) and one primary hydroxyl (C-6) as can be seen in Fig 1.1. Those hydroxyl groups form intramolecular hydrogen bonds with one another that give cellulose its unique structural characteristics. The ether bond and the hydrogen interactions force an alternating pattern in glucose units of the cellulose. Each ring is "upside down" from the last, which allows the C-6 hydroxyl of one glucose ring to interact with the C-2 hydroxyls on either side of it. This also exposes the ring oxygen of each glucopyranose ring to the neighboring C-3 hydroxyl. These interactions (Fig 1.2) give cellulose a rigid and fixed ribbon-like

structure. These interactions are only absent after chemical treatment disrupting the bonds, or at the ends of cellulose chains.

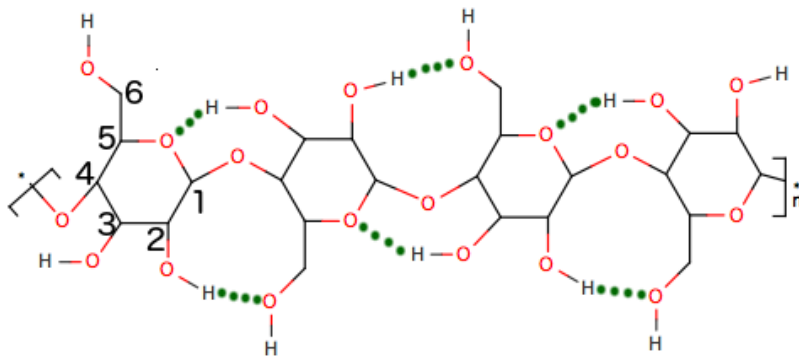


Fig 1.2: Cellulose molecule. Dotted green lines show intramolecular hydrogen bonds responsible for rigidity in cellulose molecules. This model does not precisely depict position of hydroxyls with respect to the ring plane.

The C-6 and C-3 hydroxyls also interact with one another across molecules to form intermolecular hydrogen bonds (As shown in Fig 1.3) that order chains together into crystalline groups of six that are called elementary fibers. These are the simplest cellulose "fibers" on a hierarchy where fibers are collections of discrete polymers<sup>4</sup>. Elementary fibers then collect into larger and larger groups in the same pattern to form cellulose fibers and strands that we ultimately observe in plant cell walls. A simplified idea of this recursive association and growth is shown in Fig 1.4. The figures shown represent only the first three structures. Much larger structures appear in nature as a result of the bundling described.

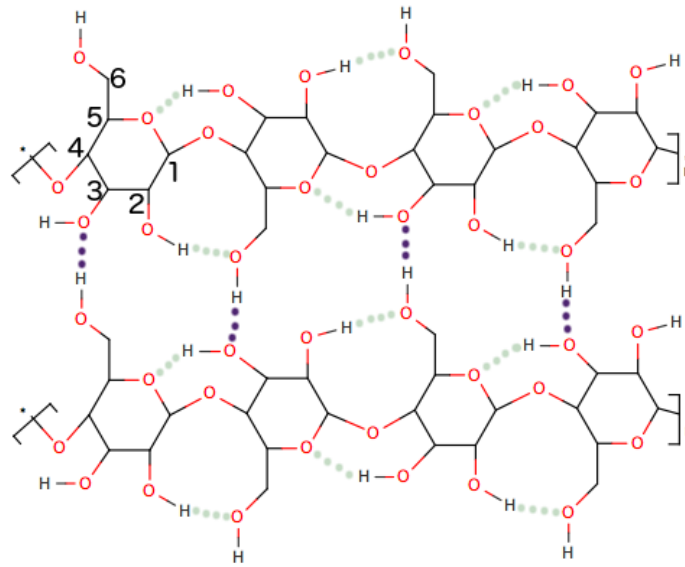


Fig 1.3: Cellulose molecules and intermolecular hydrogen bonds (purple dotted lines) between C-3 and C-6 hydroxyls.

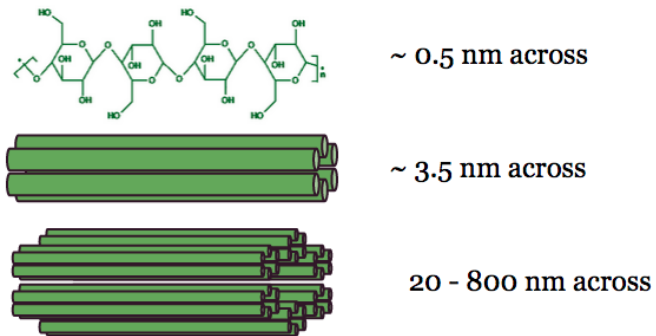


Fig 1.4: Width of cellulose complexes. Green cylinders represent single cellulose strands shown in structure above. Length values pictured represent approximate diameters of structures.

### 1.3 Nanocellulose

Those structures shown in Fig 1.4 show only fibers that have diameters less than 1  $\mu\text{m}$ . With any dimension measured in the nano range ( $1 \text{ nm} < x < 1 \mu\text{m}$ ), the structure is considered nanocellulose. Nanocellulose can be prepared in a number of ways that determine the characteristics of the final material. There are three types of nanocellulose that are of specific interest to current research<sup>5</sup>. These materials are all composed only of cellulose, differing only in characteristic dimensions.

Nanofibrillated cellulose (NFC) comprises a large distribution of dimensions. NFC usually begins as wood pulp and is further processed through either physical means such as milling, ultrasonication, or cryopulverization, or through chemical treatment with acid to disrupt intermolecular hydrogen bonding<sup>5</sup>. The result is bulk cellulose spanning the nano and micro scale, lacking precise uniformity. While this results in a product that may be difficult to work with, it is generally the cheapest and easiest material to source and produce because it can be obtained from plant fibers<sup>6</sup>. The work described in this project to be described was done using NFC.

Bacterial nanocellulose (BNC) is a form of cellulose produced via bacterial synthesis. The cellulose chains are a result of the bacterial metabolic process. Because of the specific bacterial process that produces these discrete fibers, they tend to be small in diameter (50-150 nm)<sup>7</sup>, of length similar to NFC, and most importantly, more uniform than NFC. Because BNC must be grown and collected from bacteria rather than harvested from already abundant materials, BNC is more costly and time consuming to produce.

Cellulose nanocrystals, or crystalline nanocellulose (CNC) can be produced from stock wood pulp. Selective hydrolysis is the premise for CNC production. Cellulose strands bundle as described above, but in those bundles, the ends of cellulose strands do not necessarily line up perfectly. The breaks in the crystalline structure create amorphous weak regions in the fiber structure. These weak regions are hydrolyzed, normally with acid<sup>8</sup> that is strong enough to hydrolyze the glycosidic bonds in amorphous cellulose, but not physically able to attack the intermolecular hydrogen bond crystal structure (because of those interactions). As a result, the amorphous regions of the fibers are broken, leaving behind the crystalline portions which are highly ordered and shorter compared to their predecessors.

#### **1.4 Applications and Reactions of Nanofibrillated Cellulose**

Nanofibrillated cellulose has innumerable potential applications. Some processes use the material as-is without any chemical reaction affecting the structure of the cellulose chains. Other processes utilize reactions with nanocellulose. Cellulose fibers and NFC have both been used unreacted as polymer reinforcements, taking advantage of the fiber nature and the high tensile strength of cellulose<sup>6</sup>. While cellulose isn't as strong or as stiff as carbon fiber, cellulose's strength and stiffness make it a very attractive structural fiber because of its natural abundance. Common materials that don't require exceptionally high stiffness or strength could be made using cellulose fibers rather than more expensive carbon fiber reinforcement. A wide range of cellulose reinforced polymer products on the market today<sup>9</sup>, many of which are structural or building materials. These

materials exhibit a large range of mechanical properties depending on their intended applications.

The nature of cellulose nanofibers can change when chemically treated. Certain reactions have been found to be widely beneficial in treating cellulose to make it interact differently with other materials, or to behave differently on its own. One of the most common cellulose reactions done in industry (though not exclusively on nanofibers) is the treatment of cellulose with acetic anhydride. This reaction is representative of a wide series of similar esterification reactions from acids or anhydrides<sup>3</sup>. The acetic anhydride reaction involves treating cellulose with acetic anhydride in any of many solvents. The solvents can alter the degree to which the anhydride reacts with the cellulose. The reaction takes place first on the C-6 hydroxyl, the only primary alcohol group of cellulose, and exclusively the C-6 hydroxyl in aqueous solution. Other solvents allow similar reactions on the C-2 and C-3 hydroxyls. Cellulose treated in water to create an acetoxy group on the C-6 (Fig 1.5) is used in making weak adhesives. These reactions are most often acid catalyzed depending on the solvent used<sup>3</sup>.

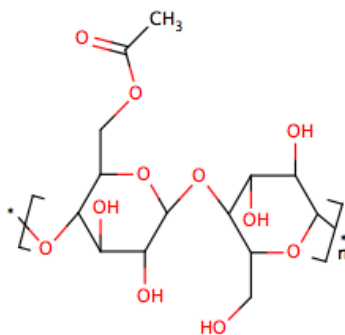


Fig 1.5: 6-acetoxy cellulose. Obtained from treating cellulose with acetic anhydride.

Similarly, cellulose fibers are treated in organic solvents in systems of acids to nitrate the hydroxyls. By treating in a mixture of nitric and other strong acids, the cellulose adopts a nitrate group in place of its hydroxyl (Fig 1.6)<sup>3</sup>. This material used to be known (and still is to some degree) as gun cotton because it could be highly explosive. It is now used in making plastics, films, and lacquers, and is only explosive at high degrees of substitution (when more than 70% of the hydroxyls are replaced with nitrate groups).

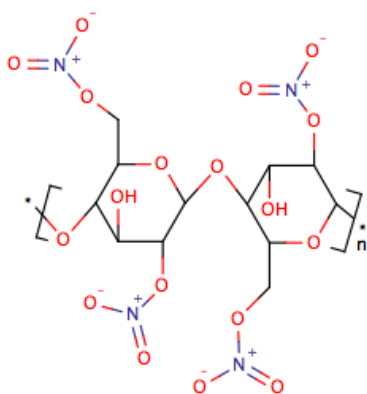


Fig 1.6: Cellulose nitrate with 66% of hydroxyl groups reacted. The remaining hydroxyls could also be reacted. The degree of substitution shown is arbitrary.

Carboxymethylcellulose (CMC) is another common derivative of cellulose. Carboxymethylcellulose is a etherified derivative of cellulose made by treating cellulose with chloroacetic acid<sup>5</sup>. The simplified reaction is shown in Fig 1.7. The resulting etherification forms a material that is commonly used as a thickening agent for industry and food as it is non-toxic and safe for consumption<sup>10</sup>. The cellulose chains become water-soluble because of the increased polarity from the pendant acetate groups and can then be used to control viscosities by its content in water.

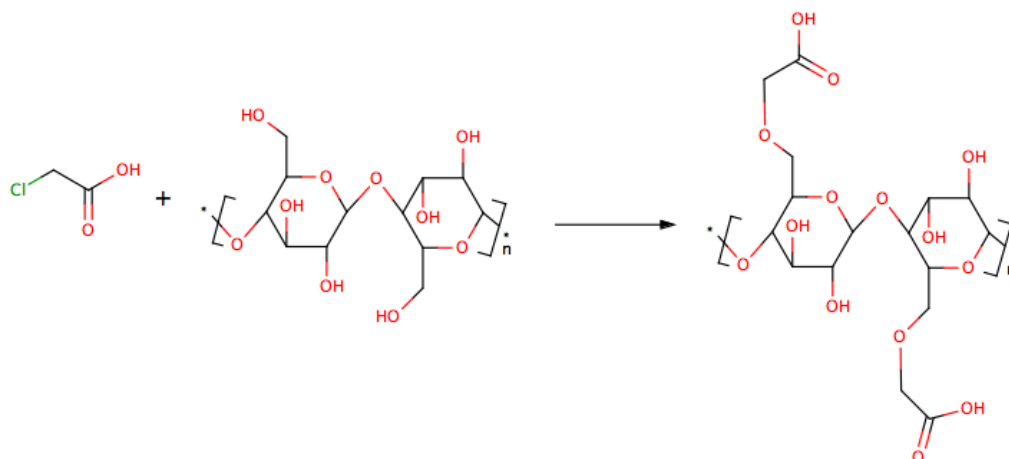


Fig 1.7: The simplified reaction between chloroacetic acid and cellulose to form CMC. In CMC, the acetate protons may be dissociated, leaving the acetate conjugate base (not shown).

One of the most common procedures used in the laboratory rather than in industry is treatment with 2,2,6,6-tetramethylpiperidinyloxy (TEMPO). TEMPO oxidation is a common method for a number of reasons. TEMPO oxidation can break down the hierarchical structure of nanocellulose to produce uniform and controllable nanofiber sizes. The oxidation process works through two steps to oxidize the C-6 carbon<sup>11</sup>. This reaction disrupts the intermolecular bonds and allows the cellulose fibers to split transversely into thinner fibers. The oxidation also functionalizes the C-6 carbon to a carboxylic acid, which has its own ability to propagate another set of reactions<sup>12</sup>. This reaction is common in the laboratory because it does not require high temperatures or pressures and is controllable by the reaction concentration<sup>13</sup>. The structure of TEMPO and the simplified reaction with cellulose can be seen in Fig 1.8.

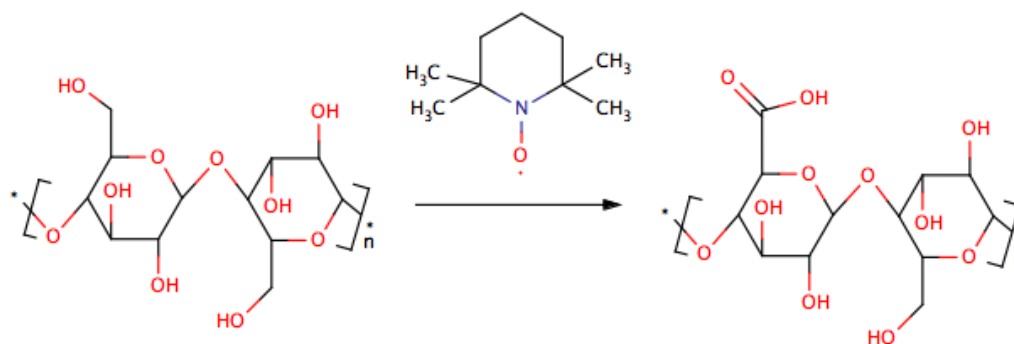


Fig 1.8: TEMPO oxidation of cellulose to form a carboxylic acid at the C-6 carbon.

While the C-6 seems to be the most commonly substituted group, this would seem to be a result of its availability. The C-6 hydroxyl is the only primary hydroxyl, which enables it to react most easily as a nucleophile<sup>14</sup>. The other hydroxyls (C-2, C-3) also have the potential to react as shown in Fig 1.6 with cellulose nitrates. Most etherifications (excepting that which produces CMC) actually take place at the C-2 hydroxyl<sup>13</sup>.

Other reactions can be done from the initial reactions on the surface of nanocellulose. Of particular interest are those reactions that can attach other polymers to functional groups on the surface of NFC. These reactions open the door to cross-linking procedures and complicated chemical process to develop very specific materials with refined properties. Several studies have been able to attach large molecules to the surface of functionalized cellulose. This includes binding DNA oligomers to the surface of CNC that had been TEMPO oxidized<sup>15</sup>. Other procedures have been successful in attaching varying lengths of polyetheramines to the surface of CNC<sup>16</sup>.

## 1.5 Motivation for This Project

The growing concern around petroleum resources has sparked a new trend towards sustainability in industry<sup>17</sup>. This has been a challenge for producers of plastic goods, the raw materials for which are often sourced from petroleum. In 2012, the average american consumed 29 lbs of plastic bottles<sup>18</sup>. While there are recycling programs in place, and while those recycling programs have been expanding over the years<sup>1</sup>, almost 70% of that material was not recycled. Despite recycling programs, biodegradable plastics that didn't have to be recycled (considering how much is recycled) would be advantageous.

Polylactic acid or polylactide (PLA), a polymer of lactide (Fig 1.9), is a material that has attracted attention as a potential alternative to polyethylene terephthalate (PET), the material that many plastic beverage bottles currently comprise. Lactide and PLA are both renewable and biodegradeable<sup>19</sup>, which make them an ideal material for consumers where recycling practices are unreliable. Those materials made of PLA will return to the environment harmlessly by decomposing if they are not recycled. In most cases, PLA can not immediately replace PET or other consumer plastics. PLA is strong, but very brittle which makes it unacceptable to the public consumer<sup>20</sup>. PLA also distorts under elevated temperature fluctuations<sup>21</sup>, which makes it unusable in an engineering environment.

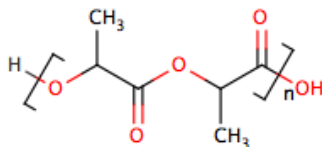


Fig 1.9: The structure of polylactic acid/polylactide

In order to use PLA as a consumer product, tougheners have been introduced, but tougheners that have worked industrially have all been sourced from petroleum<sup>22</sup>. While petroleum-sourced tougheners allow PLA to come to market, offering an improvement, they don't solve the problem posed. Finding toughening agents that effect a useful change in PLA that are also biodegradable and renewable is an active field of interest. This often involves new manners of introducing toughening polymer compounds to a bulk PLA<sup>23</sup>.

Polyisoprene, a major component in natural rubber<sup>24</sup>, could provide decent toughening properties to PLA. But introduction of polyisoprene in PLA is difficult given polyisoprene's non-polar structure (Fig. 1.10) and PLA's polar structure, making the two materials immiscible in one another. As a result of their mixtures of PLA and polyisoprene then may not be stable over time.

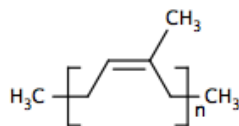


Fig 1.10: The structure of polyisoprene.

A novel manner of potentially mixing PLA and polyisoprene would be through the use of nanocellulose. NFC's aid in emulsification on their own, but by treating the surface of a nanocellulose fiber and creating a material to which polyisoprene or polyisoprene-PLA block copolymers could be grafted (Fig 1.11), the introduction of polyisoprene may be beneficial. In order the prepare this material, the cellulose must first be treated to add the necessary functional groups to attach those polyisoprene and polylactide structures.

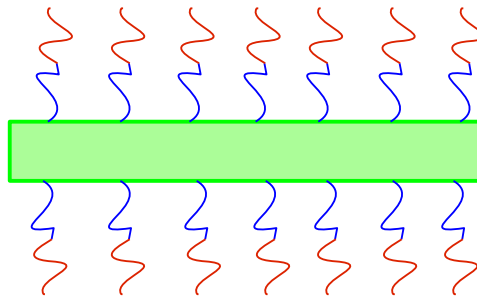


Fig 1.11: A cartoon depicting the structure of a cellulose nanofiber (green) that has been treated so that polymers of polyisoprene (blue) and PLA (red) could be grafted to the surface.

Between the emulsion aiding aspects of cellulose to help polyisoprene dispersion, the fiber-like nature of the cellulose, and the covalent bonding that would force an amount of dispersion of polyisoprene throughout a bulk PLA, a cellulose core-shell structured toughener could provide the properties required for consumers in the final PLA product. Further, a structure assembled like the core-shell would be a free-standing additive that could be added separately to a bulk material.

### **1.6 This Project**

This project will be the first step in developing cellulose-core polyisoprene/PLA-shell copolymers. A similar reaction to those esterifications described above will be implemented to react the surface of nanocellulose fibers with methacrylic anhydride and attach methacrylate functional groups to the fiber surface. The methacrylation reaction will consist of reacting varying concentrations of methacrylic anhydride in a basic aqueous environment with NFC (Fig 1.12). Methacrylic anhydride was chosen for the C=C carbon carbon double bond that can be seen in the reaction shown in Fig 1.12.

Water was chosen as a reaction medium because of the water suspended state of the available NFC.

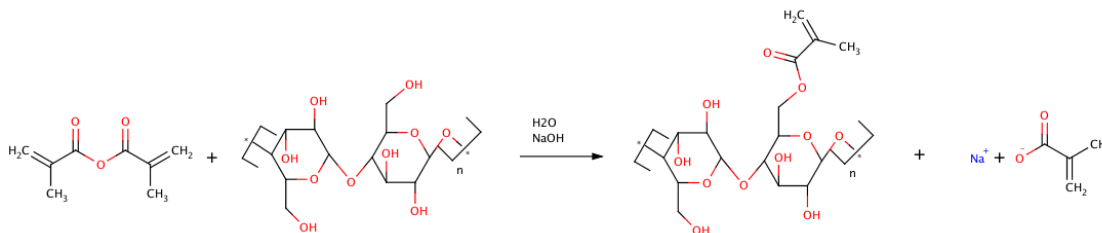


Fig 1.12: The simplified reaction between methacrylic anhydride and cellulose to form a methacrylate functionalized cellulose polymer.

Concentrations of methacrylic anhydride will be varied to observe the effects of reactant concentration on the final product. The goal will be to determine differences in degrees of reaction that can be associated with reactant concentrations. Infrared spectroscopy will be used to determine the relative degrees of reaction in each reacted sample. Infrared spectroscopy will not determine specific concentrations of any functional groups on the cellulose surface, but it will provide arbitrary relative values for all reaction conditions that can be compared to each other. The results will hopefully help form a model that can be used to control the properties of the product. Determining the degree of functionalization of the functionalized cellulose is crucial to properly inducing further reactions.

## 2. Experimental Methods for Functionalized Cellulose

### 2.1 Materials

Nanocellulose suspension in water (2.3 wt %) was acquired from the Process Development Center at the University of Maine Chemical Engineering department. The material had a distribution between about 100 nm up to 3  $\mu\text{m}$  across as seen by micrograph in Fig 2.1<sup>25</sup>, with less than 10% of fibers measuring greater than 1  $\mu\text{m}$  across. Methacrylic anhydride was purchased from Sigma-Aldrich and used without further purification. Solid sodium hydroxide pellets were purchased from Fischer Scientific and mixed with in-house-sourced deionized water to form a 10 M solution.

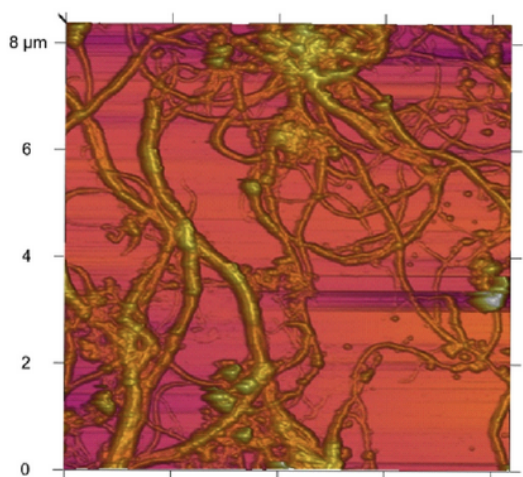


Fig 2.1: An atomic force micrograph of the starting material provided by Dr. Doug Bousfield of the Chemical Engineering department at the University of Maine <sup>25</sup>

Regenerated cellulose dialysis tubing with a 6000 - 8000 nominal molecular weight cut-off was purchased from Fischer Scientific for purifications. An Agilent 3200P pH meter was used to monitor the pH of the solutions. A 4.5 L Freezone bench-top lyophilizer from Labconco was used for all freeze-drying with Labconco 600 mL

Complete Fast-Freeze flasks. An Isotemp 281A vacuum oven was used on several occasions for further dryings.

Deuterium oxide (D<sub>2</sub>O) purchased from Acros Organics with an advertised 99.8% purity and used to conduct proton NMR for analysis of water soluble materials in a 400MHz Varian NMR with a 5mm 4-nucleus standard probe.

## **2.2 Functionalizing Nanocellulose Workup**

Typical experiments started with 100 mL of 1 weight percent NFC comprising 56.5 mL DI water and 43.5 g stock 2.3 weight percent NFC. NFC suspensions were placed in a 200 mL beaker on a stir plate and stirred with a magnetic bar. The pH probe was placed in the reaction vessel and the suspension's pH was adjusted with a drop or two of 10 M hydroxide solution to bring the pH to within 10.5 and 11.5. Methacrylic anhydride was then measured out either in a graduated cylinder or by micropipettor, depending on necessary volume, and added all at once to the NFC suspension. Three batches were made of each condition using 2 mL, 4.5 mL, 9 mL, and 18 mL of methacrylic anhydride.

Using a disposable transfer pipette, sodium hydroxide solution was added dropwise to the reaction to maintain the pH in the desired window – between 10.5 and 11.5 throughout the course of the reaction. This process continued until the rate of the pH decline required less than a drop of hydroxide solution every 20 minutes or so to maintain the desired range, reasoning that once the pH declined slowly, little reaction was still taking place. While those experiments with the smallest portions of methacrylic anhydride had the shortest reaction time to reach slow pH changes, they were allowed to

proceed for at least one hour before stopping while the experiments using the most methacrylic anhydride took just over two hours to reach the same rate of decline.

Each condition was repeated three times for three separate batches of each. From each of the three batches, three separate samples were used for FTIR spectroscopy to avoid anomalies picked up from the spectrometer that could have been atmospheric, local contaminant, or other non-characteristic disruptions.

### **2.3 Control Nanocellulose Work Up**

To compare the functionalized samples, control cellulose suspensions were produced by simply diluting the 2.3 wt % cellulose into 1 wt % suspensions and allowed to sit and stir for roughly an hour. To another control group, 1 wt % suspension was prepared as described, but two drops of NaOH solution were added to bring the pH of the suspension to just under 12. This was allowed to mix for two hours.

After mixing for the allotted time, the unreacted control cellulose was collected and placed on dialysis under similar conditions as reacted cellulose.

### **2.4 Dialysis, Freeze-drying, Preparation for FTIR**

After the reaction period, suspensions were removed from the stir plates and poured into regenerated cellulose dialysis tubing (Fischer Brand, 50mm) and placed in a four liter beaker of deionized water. A 20 mL sample portion of each reaction was saved in a sample vial as-is and refrigerated.

Samples that were determined via infrared spectroscopy to need further purification were re-suspended and returned to dialysis. About 0.2 g of dried impure cellulose product was added as a single piece to about 40 mL of deionized water. A stir

bar was added and stirred vigorously for about 40 minutes. Over this time, most samples thoroughly re-dispersed and resembled the original suspension, though more dilute. In several samples, small portions of cellulose remained clumped. These clumps were pulled apart by forceps and then allowed to mix with the rest of the solutions.

Samples were left on dialysis for at least four days over which water was changed at least six times or on a continuous flow apparatus. The continuous flow apparatus allowed about ten liters of DI water to flow over the sample over the course of a day.

Samples were then removed from dialysis and poured into ice cube trays and allowed to freeze overnight at  $-20^{\circ}\text{C}$ , forming between five and eight frozen cubes of each sample. Ice cube trays were used to increase the surface area of the frozen suspension and accelerate the freeze-drying process. These cubes were then placed on a Labconco lyophilizer in Labconco flasks set to  $-50^{\circ}\text{C}$  and  $<0.2$  mbar(g). Samples were left for two days and allowed to freeze-dry. Once dried, samples were removed from the lyophilizer and stored in either plastic bags or glass sample jars in a dark freezer until analyzed by FTIR.

## **2.5 Water Adsorption Effects on NFC and FTIR**

A second control NFC sample was prepared identically to that discussed described in section 2.3. After removing from the storage freezer and before collecting IR spectra, the cellulose was placed in a vacuum oven between  $-80$  and  $-100$  kPa gauge and  $50^{\circ}\text{C}$  and left over night.

On removal from the vacuum oven, the sample was sealed in a glass jar and three FTIR spectra were taken immediately. Subsequent IR spectra were taken leaving the

cellulose exposed to air for 20, 50, and 130 min where it was exposed to the atmosphere. After those measurements taken from atmospheric influence, the cellulose was suspended over warm water on a hot plate (~70°C) for 80 min and another series of spectra were taken. After those samples were analyzed, the cellulose was replaced to suspension over the hot water bath and a larger inverted beaker was placed over the entire system to enclose any water vapor. After 15 minutes in saturated environment, the cellulose was sampled via FTIR for a final time.

## **2.6 Contaminant Isolation**

To identify certain contaminants as discussed later, material with a particularly high suspected contamination was used to isolate the unknown compound. Three samples of the more-highly contaminated compound (As determined by FTIR integrations to be discussed) were placed into 1 mL microcentrifuge tubes. The sample tube was filled with about 0.7 mL of half-packed cellulose material. Circa 1 mL of DI water was added to each microcentrifuge tube and all were sealed.

The three microcentrifuge tubes were fastened to a vortex mixer and allowed to shake vigorously for about one hour. The tubes were then removed from the mixer and placed in a centrifuge for a total of 30 minutes at 900 xg. After the material was sufficiently separated, the supernatant was decanted from the cellulose using a glass transfer pipette and placed into new microcentrifuge tubes.

The new microcentrifuge tubes containing the supernatant were placed in the freezer overnight at -20°C. They were then placed on the lyophilizer over another night

and allowed to dry. The tubes containing dry material were placed in a dark freezer for storage.

To collect material for analysis, just over 1 mL of deuterium oxide ( $D_2O$ ) was added to one microcentrifuge tube. That tube was fastened to a vortex mixer and shaken vigorously for five minutes. The solution was transferred by glass transfer pipette to the next microcentrifuge tube. The second tube was then shaken vigorously as the first and the solution was transferred to a third tube where the process was repeated.

The final 1 mL solution containing the water-soluble contaminant was moved to a 5mm NMR tube via glass transfer pipette and analyzed as proton NMR in  $D_2O$  without further dilution. NMR conditions were set at 16 transients with a TPWR of 55, delay time of 10 s, acquisition time of 1 s, and a pulse width of 13  $\mu s$ .

## **2.7 FTIR Analysis and Integrations**

For each batch of nanocellulose prepared, three attenuated total resistance (ATR) FTIR spectra were recorded for analysis. These three spectra were all scans from only slightly different regions of the same material.

Infrared spectra were recorded using an attenuated total reflectance infrared apparatus. Cellulose was pressed against a crystal with a spring-loaded plunger that maintained pressure. Spectra were recorded in % transmittance.

Using Apache OpenOffice Calc, transmittance values were transformed to absorbance values using the equation  $A = 2 - \log(\%T)$  where  $A$  is the absorbance value, and  $\%T$  is the transmittance percent observed, in order to transform the data acquired to the linear scale of absorbance to make measurement comparisons. After

converting to absorbance, a macro was used to integrate two sets of peaks: a set reference peaks that should not change between reaction conditions as an internal standard, and a set of measurement peaks to represent the reaction. These peaks were then presented as ratios of integration values (measured to reference) to compare results from different conditions.

### **2.7.1 Integration Macro**

The macro used first converts % transmittance to absorbance. Then, prompts the user for peak ranges, first for the reference range and then the measuring range. The user enters the low and high wavenumbers for each peak span over which to integrate. Reference and measurement peaks varied slightly from batch to batch, but reference peaks were generally from about  $830\text{ cm}^{-1}$  to  $1220\text{ cm}^{-1}$  and measurement peaks were from about  $1550\text{ cm}^{-1}$  to  $1830\text{ cm}^{-1}$  as shown in Fig 2.2.

The program first uses trapezoidal rule to integrate the area between the given wavenumbers. In IR data as recorded by the instrument, each wavenumber is recorded as a point. A span of 201 points then becomes an integration of 200 trapezoids. Integrations are done from the absorbance value to the zero point. To correct for baseline curve, the integrators then subtracts a trapezoid calculated between the start and end wavenumber absorbances and the zero line as shown in Fig 2.3.

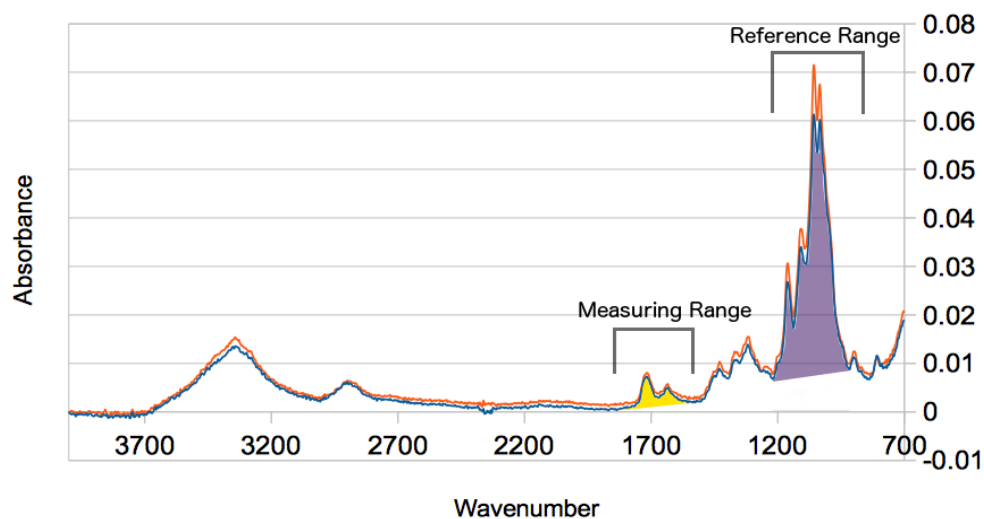


Fig 2.2. A sample absorbance IR graph. Measured peaks are shaded in yellow. Reference peaks are shaded in purple.

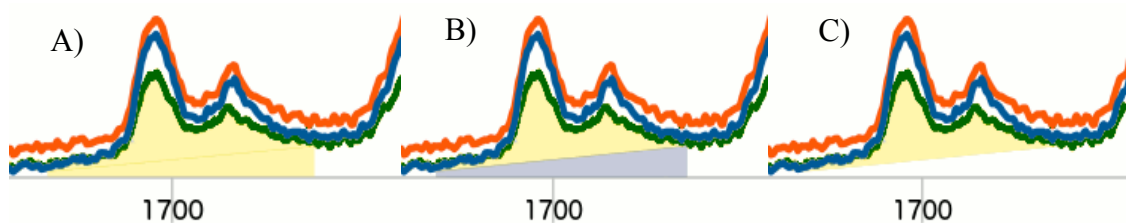


Fig 2.3. Close up of an integration peak depicting integration technique on the green series. (A) The yellow region is originally integrated by trapezoidal rule. (B) The second baseline – the blue region – is subtracted from that area. (C) The final area is corrected.

### 2.7.2 Peak Height Analysis

Few spectra were analyzed using peak height as a metric. To determine the peak heights, the absorbance FTIR spectra were used. The same border conditions used for

peak integrations were used to draw a baseline from which the peaks would be measured. The peak absorbances were then calculated less the baseline and compared.

Peaks chosen were the most significant peaks at the greatest wavenumbers. For the peaks appearing after reaction, the peak height measured was the peak near  $1720\text{ cm}^{-1}$ . The reference peak was that near  $1055\text{ cm}^{-1}$ . These were the largest peaks (and therefore most easily measured) representing the added functional group and the Once the peaks heights were calculated, the ratio between the product peak height and the reference peak height was reported as the relative peak heights (Fig 2.4).

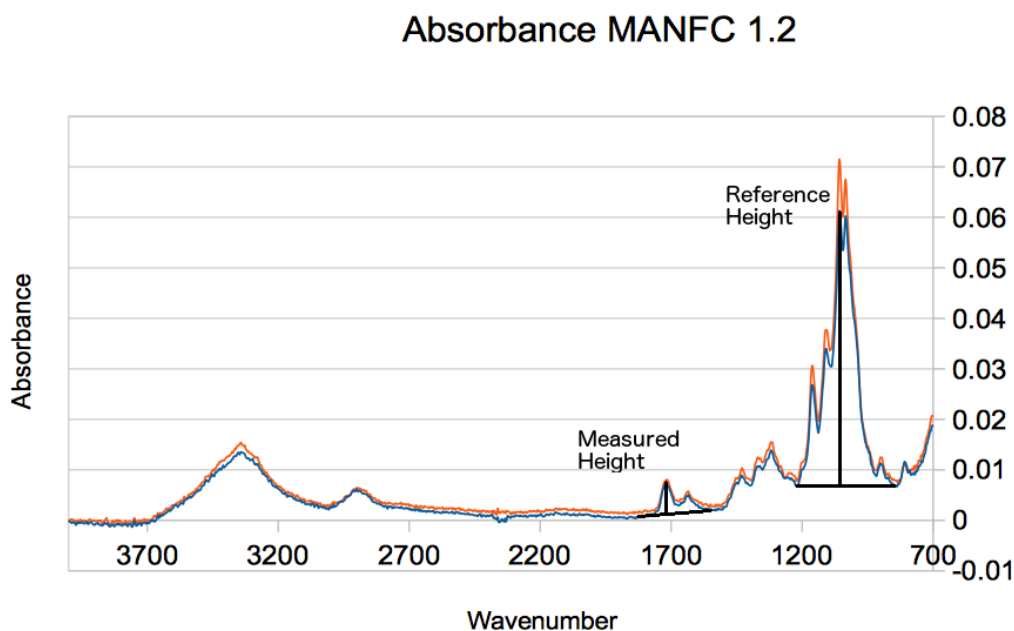


Fig 2.4: FTIR spectrum shown calculating the relative peak height between the product and reference peaks of the blue sequence in sample 1.2. The ratio between “measured height” and “reference height” is reported as relative peak height of the blue series. The points to derive the baseline subtracted from each height are the same as those used in integration analysis.

### **3. Results and Analysis**

Results for the reaction and functionalization of nanocellulose are based primarily on interpretations of infrared spectra. The concentrations prepared and those integrations performed are summarized in Table 3.1. FTIR was chosen because a specific type (attenuated total reflectance - ATR) is especially useful for investigating surfaces. Since cellulose is not easily soluble in any simple or readily available solvents, ATR FTIR was chosen as the primary investigation tool. ATR FTIR is also ideal because the reaction of interest should be occurring on the surface of the material, not in the body of the fibers. IR will likely penetrate up to a  $\mu\text{m}$ , but the surface - the area of reaction - is represented<sup>26</sup>.

Functionalization of Cellulose				
Sample	1	2	3	4
[MA ah] mM	60.0	30.0	13.0	120.0
1.1	0.0654	0.0319	0.0154	0.0565
1.2	0.0710	0.0242	0.0238	0.0541
1.3	0.0615	0.0420	0.0159	0.0541
Avg 1	0.0660	0.0327	0.0184	0.0549
Stdev 1	0.0048	0.0090	0.0047	0.0014
95% CI 1	0.0069	0.0128	0.0067	0.0020
2.1	0.1027	0.0341	0.0251	0.1279
2.2	0.0940	0.0486	0.0266	0.0836
2.3	0.0692	0.0541	0.0293	0.0875
Avg 2	0.0886	0.0456	0.0270	0.0997
Stdev 2	0.0174	0.0103	0.0021	0.0245
95% CI 2	0.0250	0.0148	0.0031	0.0352
3.1	0.0887	0.0503	0.0319	0.0732
3.2	0.0614	0.0460	0.0433	0.0788
3.3	0.0559	0.0500	0.0390	0.0638
Avg 3	0.0686	0.0488	0.0380	0.0719
Stdev 3	0.0176	0.0024	0.0057	0.0076
95% CI 3	0.0252	0.0034	0.0082	0.0109
<b>Avg all</b>	0.0744	0.0424	0.0278	0.0755
<b>Stdev all</b>	0.0165	0.0101	0.0094	0.0234
<b>95% CI all</b>	0.0127	0.0078	0.0072	0.0180

Table 3.1: A summary of conditions tested and peak integrations observed. Conditions are organized in columns with molarity in the second row just below condition number. Subsets (batches) are in the ensuing rows. Each section of three numbers in one column is one batch prepared at those conditions: the red highlighted cells for example are three samples of batch 1.1. The green highlighted cells are samples of batch 2.2. etc. So the blue highlighted cell is measurement 1 of sample 3.3, or 3.3.1. Each value is that sample's integration value after final purification.

More complicated solvent systems are available for dissolving cellulose. Dissolving the product in a system of solvents would allow the use of NMR, but these systems generally involve functionalizing the material in some way. It was decided not to pursue this method of characterization in order to avoid the further reaction of the groups of interest.

FTIR can be displayed in both absorbance or transmittance. The infrared spectrometer used reports data in transmittance. In order to quantify measurements in the manners described in the experimental section, Absorbance values were calculated from transmittance values in order to compare materials between conditions using absorbance's linear scale. In other cases that didn't require quantification, the native data was used in transmittance for simple qualitative comparison.

The spectra show similar materials, but the ranges of absorbance for the reference peaks vary from 85% to 70%. Two of these spectra are shown in Fig 3.1. This is a function of the macrostructure of the material and its contact with the ATR crystal, not of the functionalization. The scales have been adjusted to show similar graphs. The measurements of interest are those values comparing peaks within the same spectrum.

### **3.1 Infrared analysis of reaction products**

#### **3.1.1 Treatment with methacrylic anhydride**

The ATR FTIR spectra of freeze-dried, non-functionalized cellulose has a wide range from about  $2900\text{ cm}^{-1}$  to  $1425\text{ cm}^{-1}$  over which no significant peaks are present (Fig 3.1). This fortunate structure makes characterization of cellulose reactions simple because it allows easy identification of new peaks.

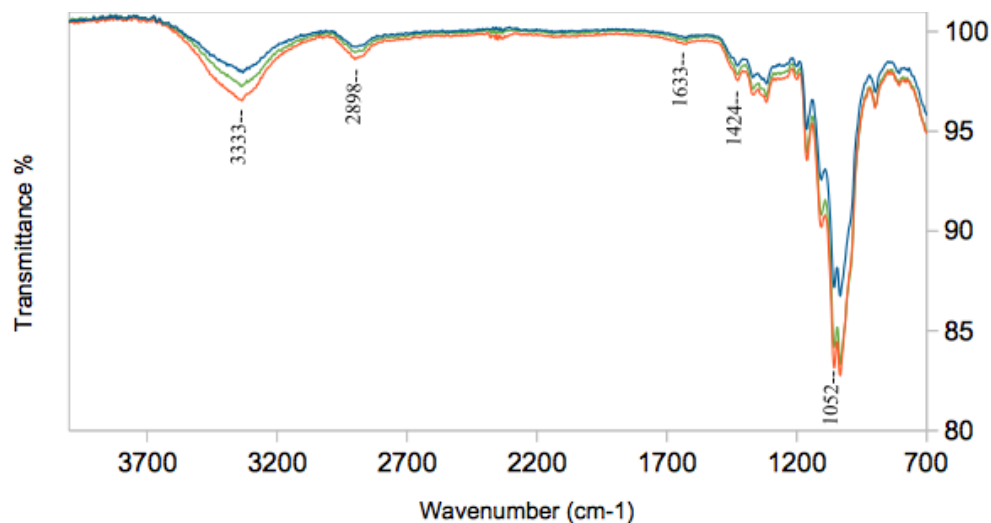


Fig 3.1: FTIR spectrum of control nanocellulose. No discernible peaks can be observed between 2900  $\text{cm}^{-1}$  and 1425  $\text{cm}^{-1}$ , save a small “hump” near 1630  $\text{cm}^{-1}$ . The three spectra reflect three different spectra taken of slightly different regions of the same sample.

Specifically, carbonyl and alkene bonds are found in this range. Methacrylate groups are indicated in the previously empty range as both a carbonyl and an alkene. When bound dilute to a surface, they show up as small peaks (by comparison to what one would normally expect from carbonyl compounds, which are often the dominant peaks of FTIR spectra), one for carbonyl near 1720  $\text{cm}^{-1}$  and one near 1630  $\text{cm}^{-1}$  (Fig 3.2) that can be attributed to the alkene<sup>27</sup>. Peaks in similar regions are seen in carboxy-methyl cellulose (CMC) where they have also been investigated with NMR<sup>28</sup>. The NMR confirms the attachment of methacrylate to CMC and suggests - given the presumption that nanocellulose and CMC behave similarly, that those peaks in nanocellulose are the result of methacrylate as well.

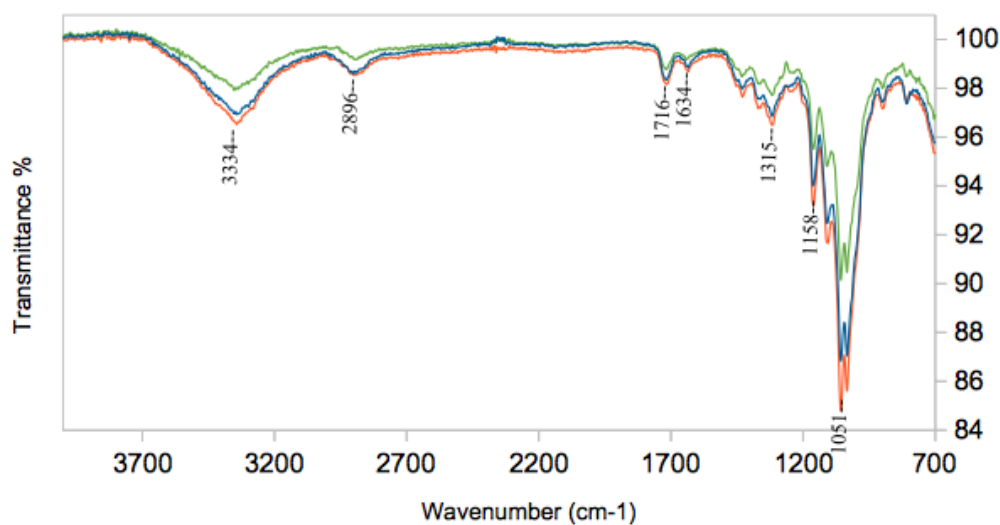


Fig 3.2: FTIR of a sample of nanocellulose reacted with 60 mM methacrylic anhydride. Two new peaks emerge at  $1716\text{ cm}^{-1}$  and at  $1634\text{ cm}^{-1}$ . The three spectra reflect three different spectra taken of slightly different regions of the same sample.

As will be discussed later, these peaks are also indicators of the extent of reaction taking place (as more bonds present will result in larger absorbances and lesser transmittances). The expectation is that larger concentrations of reactant, or at least varied reaction conditions of some sort, should result in greater extents of reaction that can be observed by infrared analysis.

### 3.1.2 Redialysis Control of Uncontaminated Material

Dialysis was investigated as a potential source of variation over samples. Similar processes were followed for each dialysis, but certain changes were made as lab space and time allowed. As a result, dialysis was considered a purification method more than a synthesis. Dialysis times were kept less consistent than other reaction factors, varying by hours or days in some cases. Some samples were left on dialysis longer than others (five

days rather than four). Some samples were purified with continuous flow dialysis while others were static.

To test the effects of extended dialysis, acceptable samples without contamination were resuspended in water and returned to dialysis. All batches reacted initially at 60 mM methacrylic anhydride were acceptable after the first round of dialysis. The material was returned to dialysis following the same methods as those returned for further purification and retested via integration after the second dialysis process. The resulting product had a diminished degree of functionalization after extended dialysis as seen in Fig 3.3.

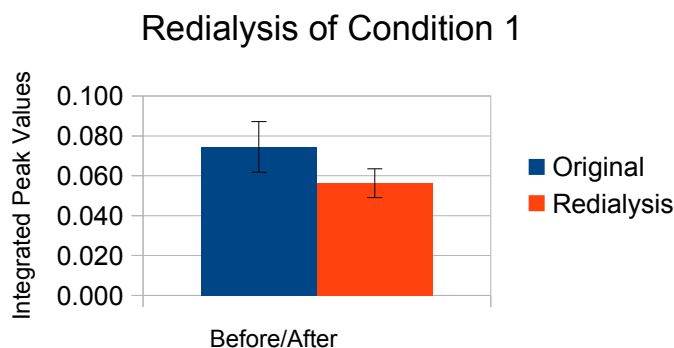


Fig 3.3: The comparison between integrated peak values for product peaks in functionalized cellulose before and after further dialysis. Error bars represent 95% confidence intervals on mean relative peak areas.

All samples measured showed decreased integration values with an average decrease of almost 22%. The loss could be a result of a number of factors including potentially different background measurements of FTIR on different days due to atmospheric conditions, but more probably were the result of hydrolysis of ester bonds.

If peak height is considered as the metric for comparing the materials, the same trend emerges. The height of product peaks less baseline as compared to the height of the reference peaks less baseline - the relative peak heights of each material - are similarly diminished by about 21% as shown in Fig 3.4.

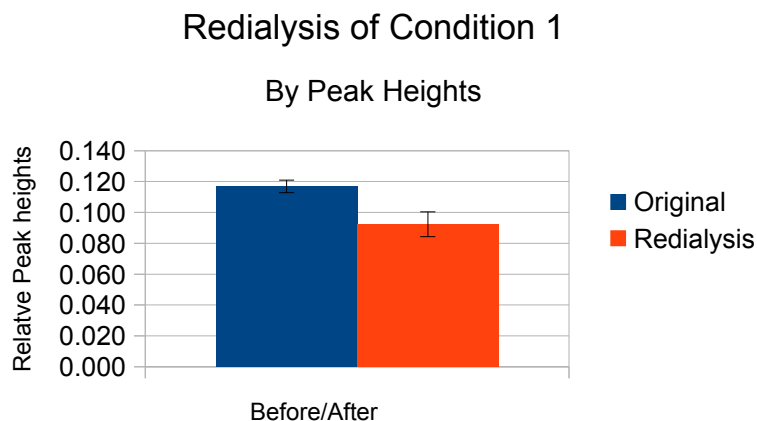


Fig 3.4: A peak height analysis of functionalized nanocellulose before and after further dialysis. Dialysis results in a diminished peak height presumably due to the loss of functional groups. Error bars display 95% confidence intervals on mean relative peak heights.

Ester bonds can hydrolyze in aqueous solution<sup>29</sup>. They would normally reach an equilibrium but using dialysis to wash away methacrylate groups would push the equilibrium towards the hydrolyzed product. According to Le Chatlier's Principle, over time, dialysis encourages the decomposition of the reacted product as collateral of purification. The changes due to dialysis are not so great so as to overcome the trend of increasing reactants leading to increasing functionalization. This also considers that those reaction conditions investigated included samples on extended dialysis.

## 3.2 Unreacted Nanocellulose

To determine the effect of treatments on cellulose, suspensions were first prepared of nanocellulose in water, dialyzed, freeze-dried, and then analyzed by ATR FTIR spectroscopy. Further steps were taken to investigate the effects of base treatments and water content of the cellulose observed by infrared spectroscopy. These experiments were conducted as a benchmark to determine the effects of other parts of the synthesis that did not include methacrylic anhydride. Their response was used to confirm that changes were the result of reaction with methacrylic anhydride.

### 3.2.1 Prepared in Base

While the reactions between cellulose fibers and hydroxide ions are well documented, and no chemically unique byproducts were expected<sup>3</sup>, only potentially shorter cellulose chains. A second control group was prepared that was first treated in base with no methacrylic anhydride for two hours. The base treatment exposed the nanocellulose to basic conditions longer than a synthesis procedure would have done. If any reactions or reaction products were observed as a result, those signs would have been more than apparent in the base-treated material.

The infrared spectra of base treated and freeze-dried nanocellulose (Fig 3.5) was not noticeably different from the freeze-dried nanocellulose without base treatments. The peaks that would normally be indicative of the product cellulose - at  $1720\text{ cm}^{-1}$  and  $1630\text{ cm}^{-1}$  - are missing. The only noticeable disturbance at  $1646\text{ cm}^{-1}$  is indiscernible from the same small hump in completely unreacted freeze-dried nanocellulose prepared without base.

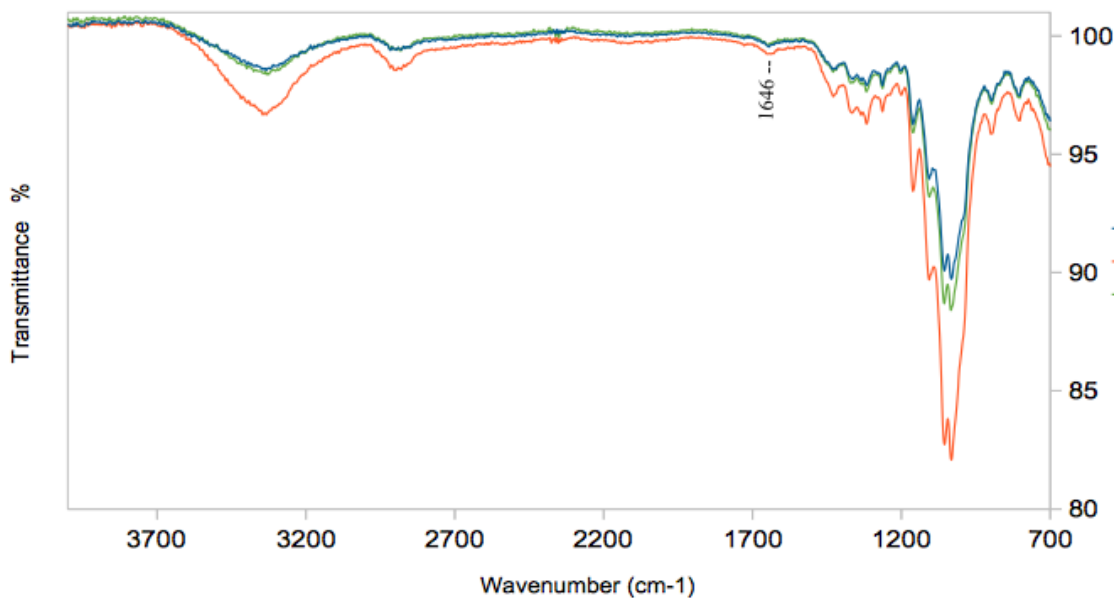


Fig 3.5: FTIR of nanocellulose after base treatment and freeze-drying without any exposure to methacrylic anhydride. No reaction is suggested in this sample. The three spectra reflect three different spectra taken of slightly different regions of the same sample.

### 3.2.2 Rehydrated by Water Vapor

Nanocellulose from the lyophilizer was expected to be "dry," but in order to investigate the effects of the minor rehydration that could occur over the course of a measurement or over the time taken to transfer material from one vessel to another. It was discovered that over time, water adsorbed to the surface of dry nanocellulose does cause a peak in the area of interest.

It is worth noting that this 15 minute time span of sitting open to the atmosphere (Fig 3.6) is more exposure to atmosphere than any other sample explicitly had. But still further measurements were taken. The small peak that can be seen to have grown at around  $1645\text{ cm}^{-1}$  grows slightly more after being left exposed to the indoor atmosphere

for another two hours and 15 minutes (Fig 3.7). This region is where the "scissor" bending mode of water is seen in pure water. After the first hour or so, the material was removed from the instrumentation room and kept desk-side in the lab office with the expectation that the environment afforded more atmospheric water to be adsorbed.

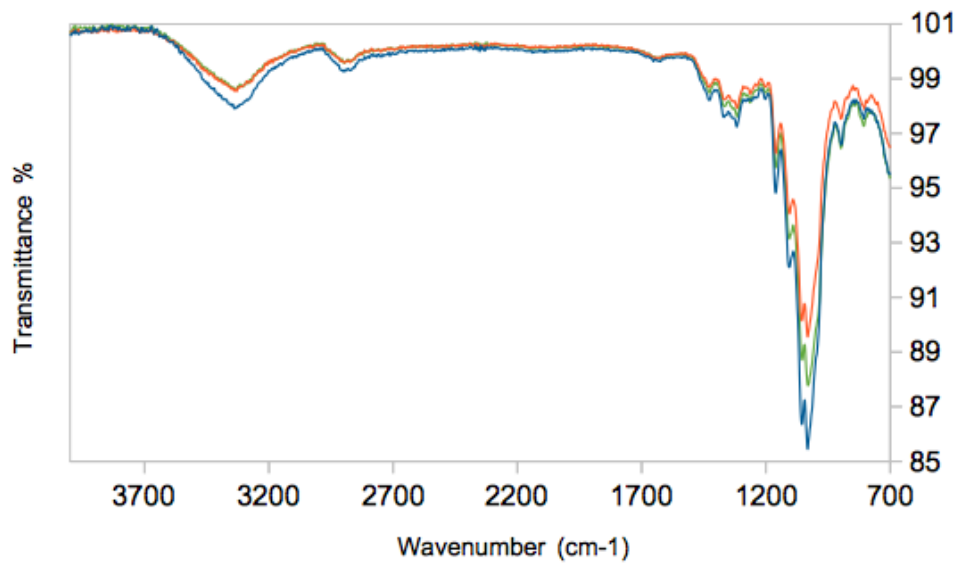


Fig 3.6: FTIR of the same control material shown in Fig. 3.1, exposed to atmospheric conditions and humidity of the FTIR instrument room for 15 minutes. The three spectra reflect three different spectra taken of slightly different regions of the same sample.

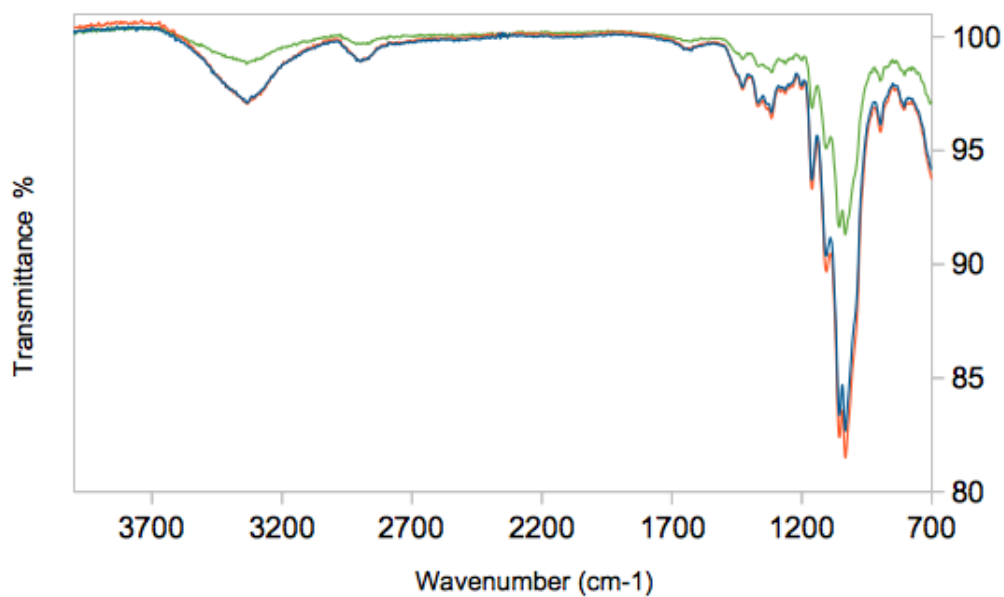


Fig 3.7: FTIR of the same material shown in Fig 3.1, exposed to atmosphere and humidity of lab office for two hours and fifteen minutes. This is much longer than any functionalized sample was allowed exposure to atmosphere. The three spectra reflect three different spectra taken of slightly different regions of the same sample.

Lastly the material was suspended over a hot water bath and a large beaker was inverted over it, effectively creating a 'sauna' environment where the atmosphere was hot and water-saturated as shown in Fig 3.8. Water vapor could be seen condensing on the inside of the inverted beaker almost immediately and after 20 minutes, water droplets had accumulated on the sides.

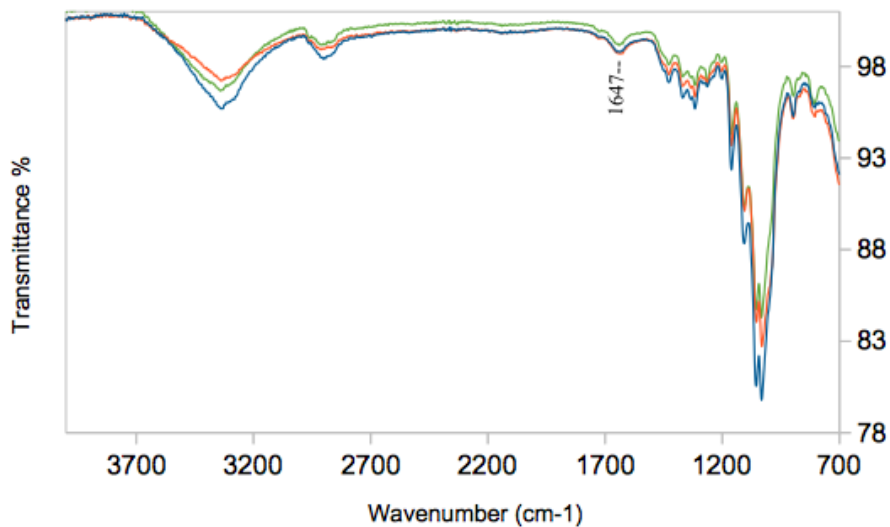


Fig 3.8: FTIR of the same material from Fig 3.7 after being exposed to water-saturated atmosphere at about 70°C for 20 min. The three spectra reflect three different spectra taken of slightly different regions of the same sample.

While water adsorption did alter the FTIR spectra in the area of interest after exposure to extreme conditions, the lesser conditions did not cause a change of the same order that would have impacted the samples. The discrepant "third peaks" - as discussed later - that were observed in the reacted materials were closer in nature to the material exposed to extremely humid conditions. Since none of those samples experienced even similar conditions, it's unlikely that water contamination was the cause, but when any materials were redialyzed to address contamination concerns as described below, they were dried again and generally analyzed more promptly. While water content was not likely responsible, the process used would have accounted for and eliminated it in taking new spectra.

### 3.3 Investigations on Contaminated Functionalized Nanocellulose

The dialysis process was more successful for some samples than for others. Certain samples prepared did feature the two emerging peaks that would be expected from methacrylate on the surface, but also a third peak at just slightly lower wavenumbers. Most divergent samples showed a third peak near  $1550\text{ cm}^{-1}$  like that shown in Fig 3.9.

#### 3.3.1 Identifying Contaminants

Those samples that showed a third peak near  $1550\text{ cm}^{-1}$ , for instance that shown in Fig 3.9, were selected for redialysis. The peaks were of varying sizes compared to the other peaks observed in the same spectra, though they were usually about the same size as the alkenyl peak near  $1630\text{ cm}^{-1}$ .

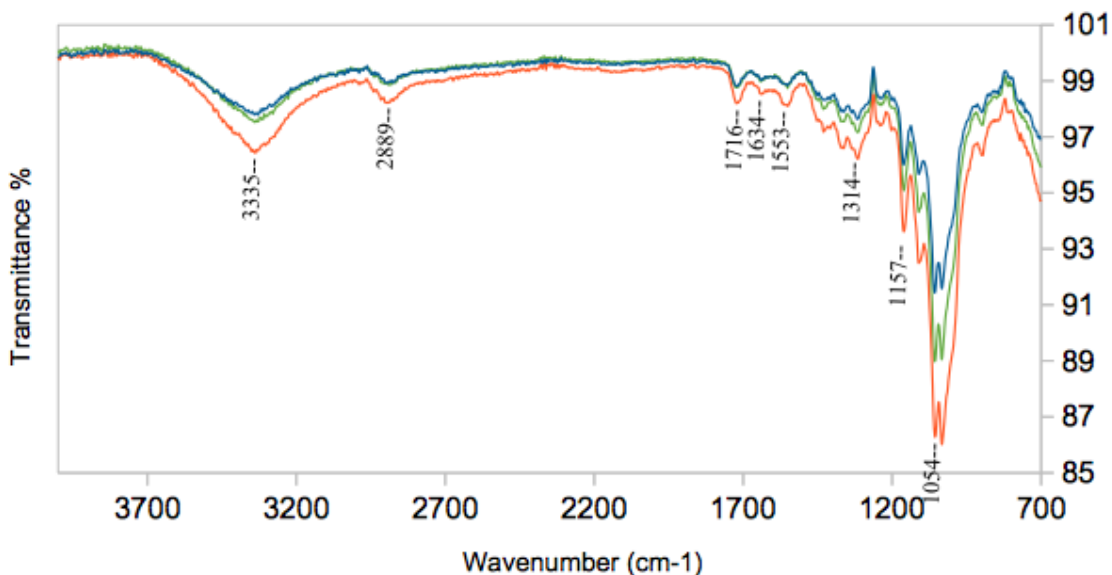


Fig 3.9: FTIR of a freeze-dried sample of nanocellulose reacted with 30 mM methacrylic anhydride. A typical “third peak” is observed near  $1550\text{ cm}^{-1}$ . This peak is present in only some functionalized products. The three spectra reflect three different spectra taken of slightly different regions of the same sample.

All reagents used were water soluble, so the expectation was that any contamination was also soluble in water as no precipitates were noticed in the samples prepared. These materials were put back on dialysis and reanalyzed after a second round of purification. This further purification yielded results much more in line with expectation by removing the third peak, leaving the two peaks that could be attributed to the alkene and carbonyl bonds as shown in Fig 3.10.

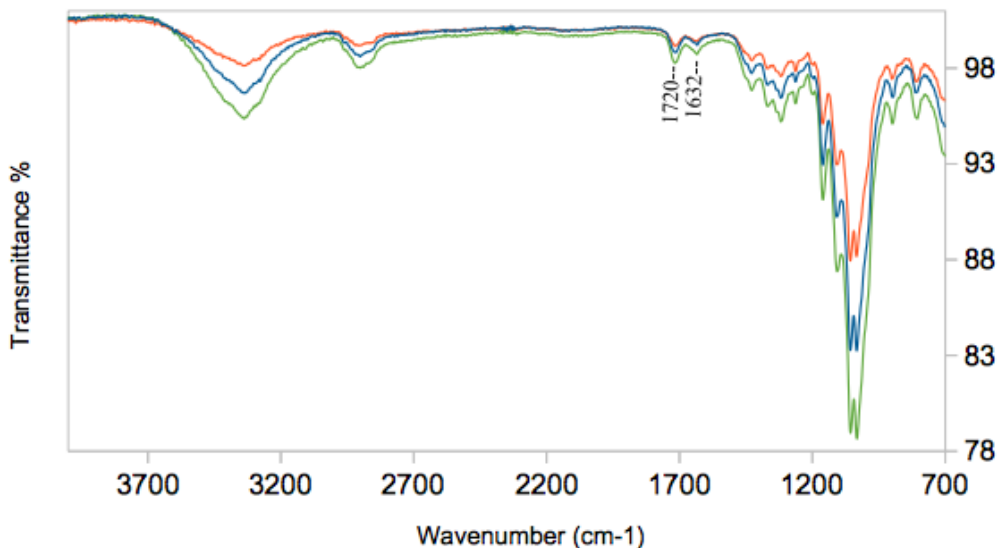


Fig 3.10: FTIR of the same materials as shown in Fig 3.9 after redialysis. The three spectra reflect three different spectra taken of slightly different regions of the same sample.

Sodium methacrylate poses a potential contaminant as the conjugate to the reaction taking place as shown in Fig 1.12. It also has a series of peaks centering around  $1550\text{ cm}^{-1}$ , indicative of a carboxylate<sup>30</sup>, according to spectra<sup>31</sup> obtained from Scifinder's database and Sigma-Aldrich.

### 3.3.2 Collecting and Characterizing Contaminants

Based on the apparent water solubility of contaminants by the ability to remove them with water dialysis, deuterium oxide ( $D_2O$ ) was used to collect contaminant from a sample prepared at 120 mM - the sample with the most contamination as indicated by the size of the  $1550\text{ cm}^{-1}$  contaminant peak. The sample was used and concentrated three times over in  $D_2O$ . It was the most contaminated sample of those prepared and using it for contaminant isolation offered the best chance to obtain a contaminant concentration great enough to analyze with HNMR.

The salt sodium methacrylate seemed the most likely to be the source of contaminant, as supported by the obtained spectra. This matches many peaks seen in spectra for 2-Propenoic acid, 2-methyl-, sodium salt from Scifinder and Sigma-Aldrich, lacking the hydroxyl hydrogen. Without that hydroxyl and leaving only sodium methacrylate, the spectra would reflect that shown in Fig 3.11. The chemical shifts resulting from the contaminant material isolated from sample 4.3 indicate that the material isolated was indeed sodium methacrylate salt. Alkane hydrogens appeared near 1.7 ppm, the trans alkane hydrogen at 5.2 ppm, and the cis alkane at 5.5 ppm.

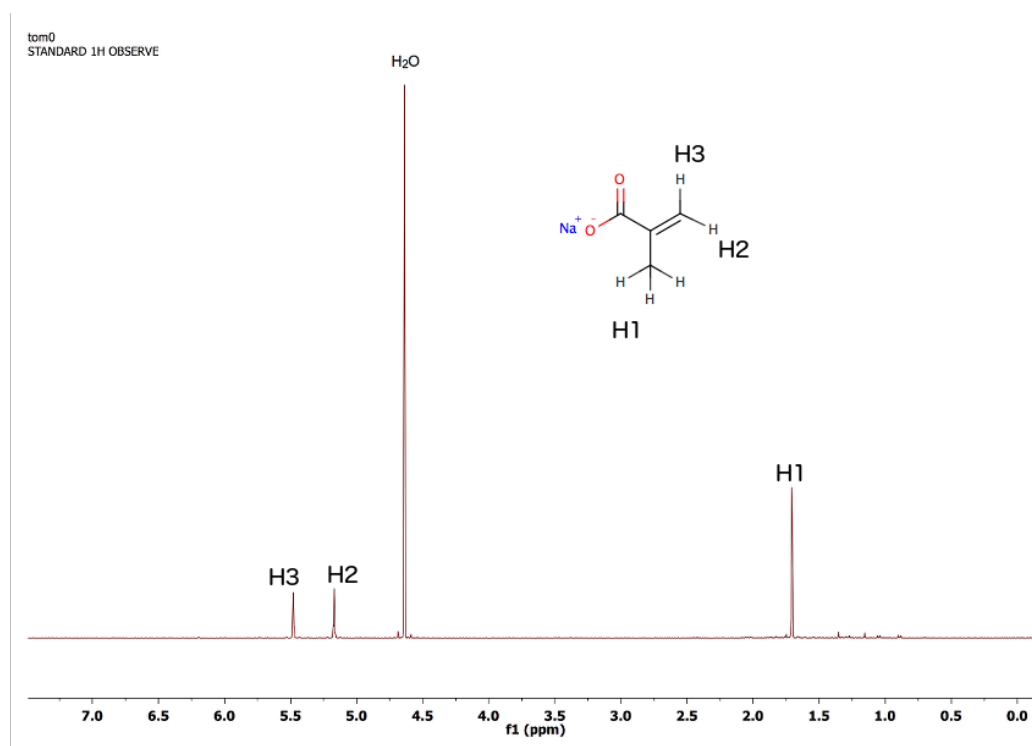


Fig 3.11: Proton NMR of contaminant isolated from functionalized cellulose 4.3. The peaks present match what would be expected from sodium methacrylate salt. The sodium methacrylate molecule is pictured with labeled hydrogen atoms corresponding to the labeled peaks.

### 3.4 Distinct Functionalized Products

Having obtained FTIR spectra of each product, each material was analyzed by integrating the two new peaks that emerged at about 1720 and 1630  $\text{cm}^{-1}$  and comparing them to integrations of the large series of peaks from the C-O bonds in cellulose between roughly 1220 and 860  $\text{cm}^{-1}$ . These integrations were done for all three samples of each batch (three batches per condition) and the relative integrations were averaged for each batch. All samples of each condition (nine samples per condition) were also averaged to compare conditions as shown in Fig 3.12. 95% confidence intervals were calculated as well to determine a predicted range for each reaction condition.

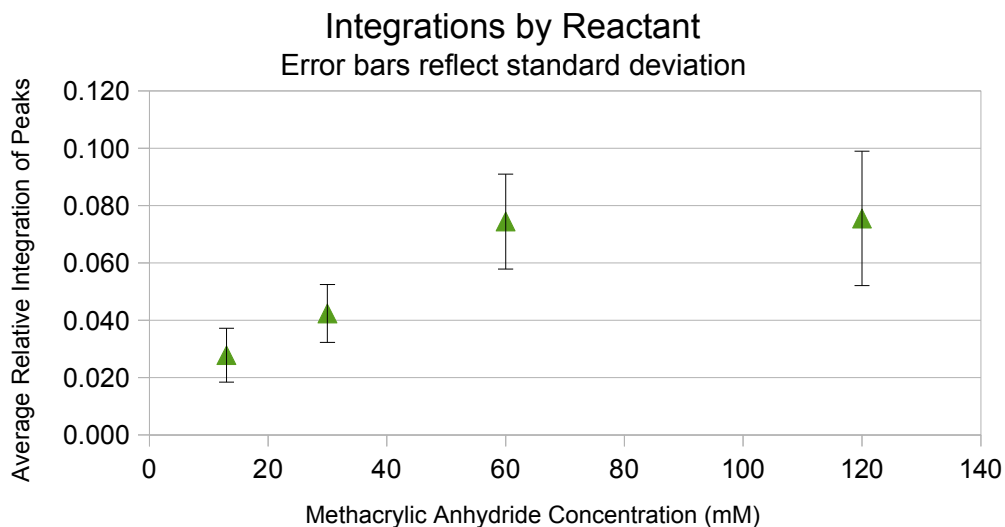


Fig 3.12: Average values of relative peak integrations as described. Values are separated by condition group. Error bars depict standard deviations within each condition.

Once standard deviations and confidence intervals were established conditions were analyzed by a student's t test not assuming equal variances - also called a welch's t test - to determine if the reaction conditions had yielded necessarily distinct materials based on what appeared to be relative functionalization. Each reaction condition's results were compared to those next conditions most similar to itself either higher or lower in methacrylic anhydride concentration. i.e. the reaction of 13 mM of methacrylic anhydride was compared to that of 30 mM; 30 mM was then compared to 60 mM, etc. The resulting trend in functionalization vaguely resembles a pattern given by the function

$f(x) = A * x / (1 + x)$  where  $x$  is the value measured and  $A$  is a constant. The decreasing slope could be indicative of a more densely populated surface as reactions progress on the surface.

Table 3.2 shows the results that the first three conditions (13 mM, 30 mM, and 60 mM of methacrylic anhydride) yielded distinct products according to the welch's t test,

but that there was not necessarily a difference between using 60 mM and 120 mM of methacrylic anhydride in reaction. Methacrylic anhydride concentration in solution has an effect on extent of reaction with cellulose up to a point where the reaction ability is exceeded.

[MA ah] (mM)	t test to compare means. (unequal variances)		
	120 to 60	60 to 30	30 to 13
$S_{x1-x2}$	0.00956	0.00647	0.00460
$v$	14.39	13.25	15.90
t calc	0.11200	4.95674	3.16681
t table	2.145	2.160	2.131
	Not Distinct	Distinct	Distinct

Table 3.2: Compares conditions of adjacent characteristics. The relative functionalization of those reactions done with 120 mM of methacrylic anhydride do not appear distinct from those done with 60 mM, but those of 60 mM are distinct from those of 30 mM, which are also distinct from those of 13 mM.

### 3.5 Other Factors

As a result of reaction conditions varying the concentration of methacrylic anhydride, other reactions conditions were not stable (Fig 3.13). Higher concentrations of the reactant resulted in extended reactions times in some cases and in higher temperatures. The temperatures could be either a result of the reactant itself or the increased amount of hydroxide added to the mixture to maintain pH.

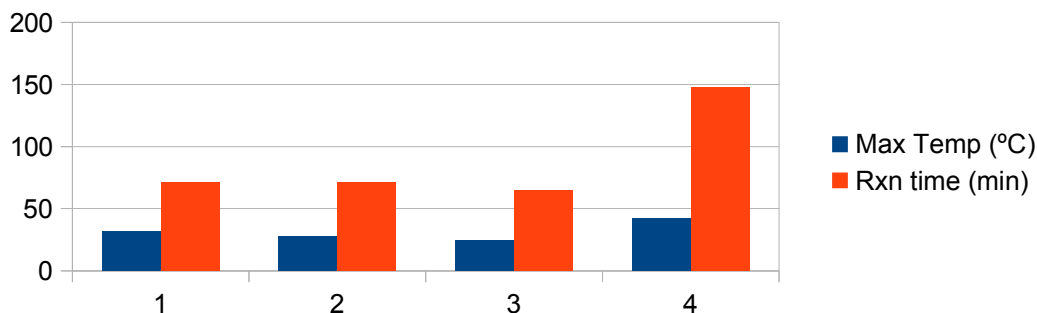


Fig 3.13: Maximum temperatures of reactions and reaction run times of reactions with varying concentrations of methacrylic anhydride. 1 = 60 mM, 2 = 30 mM, 3 = 13 mM, and 4 = 120 mM

### 3.5.1 Time Reacted

Reaction time was a function of pH drop. The reaction was allowed to continue until the pH of the reaction solution was dropping slower than about one pH unit every twenty minutes. Water reacts with methacrylic anhydride to form methacrylic acid (Fig 3.14) in addition to the reaction with nanocellulose. As more methacrylic anhydride is used, the pH drops more. The increasing trend of reaction time to methacrylic anhydride concentration as shown in Fig 3.15 would make it seem as though as the reaction time increases, the extent of reaction also increases.

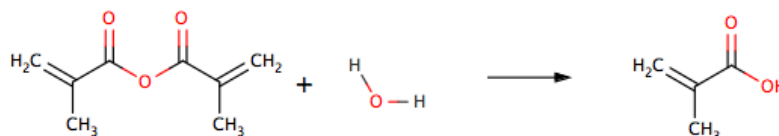


Fig 3.14: The side reaction between methacrylic anhydride and water to form methacrylic acid, accounting for the pH drop observed in the reaction procedure.

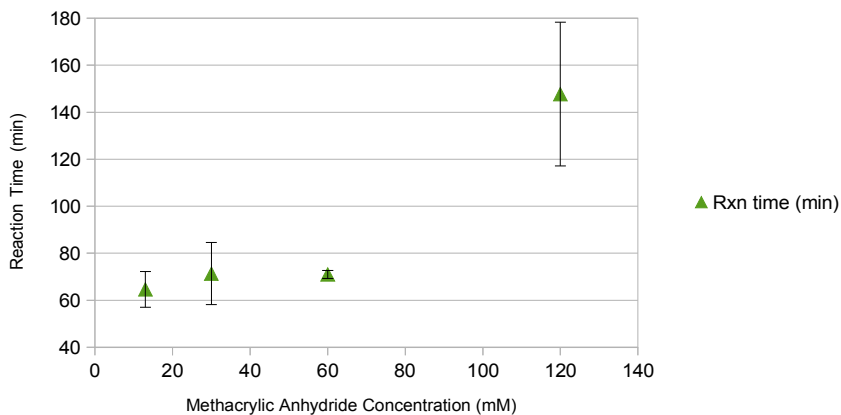


Fig 3.15: Plot of average reaction time as a function of reaction concentration. Error bars represent standard deviations of reaction times.

While extent of reaction may seem to increase with reaction time, any trend observed are more likely a result of these being byproducts of reaction concentrations. As it takes longer for water and base to neutralize methacrylic anhydride, these reactions are only allowed to "progress" for longer periods of time. Based on the observations above of a plateau, the material is more likely to have finished reacting at higher temperatures and the other reagents are simply progressing through side reactions. While there likely is some kinetic/time requirement of this reaction, it is probably achieved before the time periods observed, so it is assumed that the surface reaction is not a result of time reacted, and only a competition with methacrylic anhydride concentration.

### 3.5.2 Reaction Temperature

Results similar to reaction time were observed with reaction temperature (Fig 3.16). more concentrated methacrylic anhydride coincided with a higher temperature reaction by either a result of reaction, side reaction with water, or dissociation of greater amounts of sodium hydroxide. All reactions increased over the course of the experiment to a maximum temperature and then cooled as pH drop slowed.

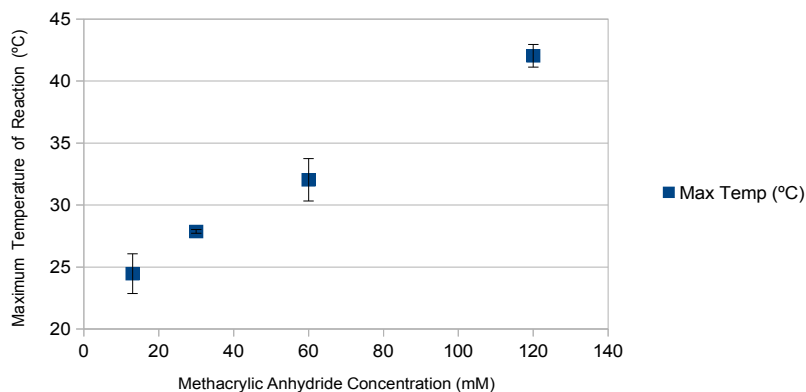


Fig 3.16: Temperature of reaction as a function of methacrylic anhydride concentration.

It's well known that as concentrated sodium hydroxide - like many other solutions - is diluted, it is very exothermic<sup>29</sup>. Just as with reaction time, more sodium hydroxide had to be added to each solution of greater methacrylic anhydride concentration in order to neutralize the products of the side reactions. As a result, extra heat was generated. If the methacrylic anhydride process was exothermic at all, that also could have contributed to the warming effect, but it is not necessary to conclude that reaction temperature directly affects reaction progression.

### **3.6 Limitations of Analysis**

In order to account for the diverse chemical environment of the bonds on which the results are based, peak integrations were used as opposed to peak heights. Peak heights may also provide useful information in certain situations where more specific properties and very specific peaks are being investigated. Peak areas are especially susceptible to contamination. Because of how the integration method works, the peaks to use for characterization need to be uninterrupted by contaminant, otherwise those contaminant peaks will distort the integrated values. Peak heights may be evaluated in the presence of some contamination so long as the peak apexes do not overlap, so the contaminant peaks won't interrupt the point at which the peak of interest is measured. Since integration accounts for the entirety of the peak body, if any part is interrupted by another peak - contaminant or otherwise - integration becomes impossible without further processing and separating peaks.

Baseline correction is a delicate procedure when investigating peak areas. Because the baseline is not expected to be consistent throughout the entire spectrum and

the background isn't necessarily stable, the baseline is accounted for as the lowest points on either side of the peaks of interest. If those low areas are obstructed or altered, the correction doesn't work properly and distorts the calculated peak area. This distortion could be the result of small variations in the measurements from the instrument, and if the backgrounds are too different between compared samples, the correction methods may actually distort results further.

### **3.7 Speculation on Reaction Extent**

There are a number of reasons why a reaction may only progress so far. The higher methacrylic anhydride concentration may force a greater extent of reaction up to a point. At that point which we will consider a maximum, the reacting surface - the nanocellulose may be saturated to a point where no more methacrylic anhydride can react for lack of reactive zones. The plateau itself might mean that all primary hydroxyls (all carbon-6 hydroxyls of surface glucose monomers) may have reacted. Those hydroxyls may instead have reacted to a point where methacrylic anhydride can no longer access the remaining hydroxyls of the same nature due to steric hindrance. Methacrylic anhydride is a rather bulky molecule and as methacrylate groups populate a surface, they may do so to a point that makes it prohibitively difficult for methacrylic anhydride to find a reaction site. The steric inhibitions would prevent further reaction once a certain portion of the available surface had been reacted.

It is also possible that an equilibrium is established between the hydroxyl groups in solution (the basic environment) and the suspension solutions. The hydrolysis

of the methacrylate group may occur at a higher rate in the reaction solutions, which could reach a point that does not allow a further degree of reaction.

## 4. Conclusions

### 4.1 Results of Experiments

Treating nanocellulose in a basic aqueous environment does functionalize the surface of the cellulose with methacrylate groups. These groups can be observed with infrared spectroscopy in the range of  $1750\text{ cm}^{-1}$  to  $1650\text{ cm}^{-1}$ . Those peaks observed grow as methacrylic anhydride concentration is increased until a certain point at concentrations over 30 mM (probably near 60 mM) where functionalization no longer increases as reactant concentration does. The trend of increase resembles one to that of the equation  $f(x) = A * x / (1 + x)$  where  $A$  is a constant, considering only reactant concentration. This may be a result of the surface becoming more populated with functional groups and less available for further reactions.

Other reaction conditions like reaction time necessary and temperature seem to be functions of the reaction pH and reactant concentration. They could also be controlled with the correct setup. When examined with otherwise identical conditions, they do not appear to affect the reaction extent, but further investigation would be necessary to confirm, as current results are not complete enough to draw any significant conclusions on these conditions.

The ester bonds between the cellulose backbone and the methacrylate groups hydrolyze in water, so extended exposure to or storage in water could degrade the final product. This degradation happens over the course of days, so purification methods that require shorter time periods would be more suited for the reaction.

## **4.2 Future Works**

This work establishes several important concepts, but more information would be helpful. The experiments discussed could be refined with more conditions and exploring other variables. The trend specifically should be investigated, as it could result in the development of a more controllable process that would allow production of a specific product. Further, this material - in whatever conditions may be produced - could be used for future reactions and development of more complicated products.

### **4.2.1 Refinement of This Process**

The trend of increasing functionalization with methacrylic anhydride concentration should be further investigated with conditions between those already investigated. Special attentions should be paid to the conditions of more concentrated methacrylic anhydride (60 mM to 120 mM) to examine the point where functionalization plateaus.

Conditions aside from methacrylic anhydride concentration should be investigated to determine an optimal environment for functionalization. Assuming an aqueous suspension, pH window, reaction time, and reaction temperature all may affect the functionalization of nanocellulose. Individual experiments for each of these conditions would be beneficial in understanding the effects of the environment on the reaction.

Other methods of purification and separation should also be investigated. As the aqueous solution seems to hydrolyze esters during dialysis, dialysis may not be the best method. A manner of immediately removing the functionalized nanocellulose from water and rinsing away contaminants would be ideal. Filtration seems like an interesting option,

but the concern arises in matting the wet nanocellulose which would be difficult to re-disperse if allowed to matt.

#### **4.2.2 The Next Steps**

Once a product is formed, the next portions of development may begin.

First, a simple reaction with the surface methacrylate groups is necessary as it proves the reactivity of the groups. While we can show that new groups appear as a result of the treatment, it would be unhelpful progress if those new groups were nonreactive with further treatments. A thiol could be used with a unique group that would show up in IR - for instance benzyl mercaptan with its aromatic ring - to react the alkenyl bond on the functional nanocellulose. Once the new groups are deemed to be reactive, other materials may be attached to the functional surface of the nanocellulose to prompt a number of properties.

Once functional, the nanocellulose may be treated to grow new polymer chains from the surface or grafted with pre-made polymer chains. The former would likely have a better result due to the kinetic interactions of the sites but the method may depend on side reactions and conditions. From there, another polymer may be blocked to the first to create the grafted material discussed previously. Interactions with that material and a bulk could then be studied to evaluate the material as a commercial additive or toughener.

- (1) NAPCOR; APR. Postconsumer PET Container Recycling Activity in 2013, 2013.
- (2) Klemm, D.; Heublein, B.; Fink, H.-P.; Bohn, A. *Angew. Chem. Int. Ed.* **2005**, *44* (22), 3358–3393.
- (3) Sjöström, E. *Wood Chemistry: Fundamentals and Applications*; Gulf Professional Publishing, 1993.
- (4) Chinga-Carrasco, G. *Nanoscale Res. Lett.* **2011**, *6* (1), 417.
- (5) Habibi, Y. *Chem. Soc. Rev.* **2014**, *43* (5), 1519–1542.
- (6) Wei, H.; Rodriguez, K.; Renneckar, S.; Vikesland, P. J. *Environ. Sci. Nano* **2014**, *1* (4), 302–316.
- (7) Zhou, Q.; Malm, E.; Nilsson, H.; Larsson, P. T.; Iversen, T.; Berglund, L. A.; Bulone, V. *Soft Matter* **2009**, *5* (21), 4124–4130.
- (8) Lu, P.; Hsieh, Y.-L. *Carbohydr. Polym.* **2010**, *82* (2), 329–336.
- (9) Bledzki, A. K.; Gassan, J. *Prog. Polym. Sci.* **1999**, *24* (2), 221–274.
- (10) Ranjbar, S.; Movahhed, S.; Nematti, N.; Sokotifar, R. *Appl. Sci. Eng. Technol.* **2012**, *4* (19), 3819–3821.
- (11) Isogai, A.; Saito, T.; Fukuzumi, H. *Nanoscale* **2011**, *3* (1), 71–85.
- (12) Johnson, R. K.; Zink-Sharp, A.; Glasser, W. G. *Cellulose* **2011**, *18* (6), 1599–1609.
- (13) Siró, I.; Plackett, D. *Cellulose* **2010**, *17* (3), 459–494.
- (14) Fox, S. C.; Li, B.; Xu, D.; Edgar, K. J. *Biomacromolecules* **2011**, *12* (6), 1956–1972.
- (15) Mangalam, A. P.; Simonsen, J.; Benight, A. S. *Biomacromolecules* **2009**, *10* (3), 497–504.
- (16) Azzam, F.; Heux, L.; Putaux, J.-L.; Jean, B. *Biomacromolecules* **2010**, *11* (12), 3652–3659.
- (17) Kaseva, M. E.; Gupta, S. K. *Resour. Conserv. Recycl.* **1996**, *17* (4), 299–309.
- (18) NAPCOR. 2012 UNITED STATES NATIONAL POST- CONSUMER PLASTICS BOTTLE RECYCLING REPORT, 2012.
- (19) Robertson, M. L.; Chang, K.; Gramlich, W. M.; Hillmyer, M. A. *Macromolecules* **2010**, *43* (4), 1807–1814.
- (20) Henton, D.; Gruber, P.; Lunt, J.; Randall, J. In *Natural Fibers, Bipolymers, and Biocomposites*; CRC Press, 2005; pp 527–578.
- (21) Bledzki, A. K.; Jaskiewicz, A.; Scherzer, D. *Compos. Part Appl. Sci. Manuf.* **2009**, *40* (4), 404–412.
- (22) Han, L.; Han, C.; Dong, L. *Polym. Compos.* **2013**, *34* (1), 122–130.
- (23) Odent, J.; Leclère, P.; Raquez, J.-M.; Dubois, P. *Eur. Polym. J.* **2013**, *49* (4), 914–922.
- (24) Greve, H.-H. In *Ullmann's Encyclopedia of Industrial Chemistry*; Wiley-VCH Verlag GmbH & Co. KGaA, 2000.
- (25) Bousfield, D. Nanocellulose micrographs, 2015.
- (26) Wessel, E.; Heinsohn, G.; Schmidt-Lewerkuehne, H.; Wittern, K.; Rapp, C.; Siesler, H. W. *Appl. Spectrosc.* **2006**, *60* (12), 1488–1492.
- (27) Moller, K.; Bein, T.; Fischer, R. X. *Chem. Mater.* **1999**, *11* (3), 665–673.
- (28) Gray, A.; Dadoo, N.; Gramlich, W. Synthesis and Characterization of Methacrylated Carboxymethyl Cellulose (MeCMC), 2014.

- (29) Smith, J. G. *Organic Chemistry*, 3rd ed.; McGraw-Hill, 2011; Vol. 1.
- (30) Cheng, S. S.; Scherson, D. A.; Sukenik, C. N. *Langmuir* **1995**, *11* (4), 1190–1195.
- (31) Hui-lu Wu. *Synth. React. Inorg. Met.-Org. Nano-Met. Chem.* **2007**, *37* (1), 57–60.

## **Author Biography**

Thomas McOscar was born in Bangor, Maine, April 24, 1992 and raised in that same city, graduating from Bangor High School, until moving to the University of Maine in August of 2010. He received Bachelor of Science degrees in chemistry and chemical engineering from the University of Maine in May, 2015. Throughout his time at the University of Maine, Thomas worked in both the engineering and the chemistry departments as a teaching assistant and also at the Maine Bound Adventure Center as a trip leader and bicycle mechanic.

Upon graduating, Thomas plans to work full time for no more than five years before returning to school to complete a Ph.D. in chemistry and materials sciences. He intends to work in research for materials design. This direction is motivated by the activities he adopted while at the University of Maine.